

Characterization of Tumor Immune Microenvironment in Meningiomas: Correlation of Tumor-infiltrating Lymphocyte Aggregates With Tumor Grade

TOSHIAKI INOMO¹, MASASUKE OHNO², TORU NAGASAKA³, SHUNICHIRO KURAMITSU⁴, EIJI ITO¹, TADASHI WATANABE¹ and MITSUGU FUJITA⁵

¹Department of Neurosurgery, Aichi Medical University, Nagakute, Japan;

²Department of Neurosurgery, Aichi Cancer Center, Nagoya, Japan;

³Association of Medical Artificial Intelligence Curation, Nagoya, Japan;

⁴Department of Neurosurgery, Nagoya Medical Center, Nagoya, Japan;

⁵Center for Medical Education and Clinical Training, Kindai University Faculty of Medicine, Osaka-Sayama, Japan

Abstract

Background/Aim: Malignant meningiomas are aggressive intracranial tumors with high recurrence rates and limited treatment options. The tumor immune microenvironment (TIME) plays a pivotal role in the tumor progression and treatment response. However, its role in meningioma remains largely unknown. This study aimed to analyze tumor-infiltrating lymphocytes (TILs) within the meningioma TIME and investigate their correlation with clinical parameters. **Patients and Methods:** Using tumor specimens from patients diagnosed with meningioma (grade 1, 12 cases; grade 2, 10 cases), the densities of CD4+ T-cells, CD8+ T-cells, CD20+ B-cells, and tissue-resident memory T-cells were quantified using multicolor immunohistochemistry and the QuPath software. The results were analyzed along with clinical parameters, including tumor grades.

Results: The density of individual TIL subsets did not correlate with the tumor grades or patients' postoperative neurological function. TIL aggregates were observed in grade 2 meningiomas; clusters of abundant B-cells with a few follicular helper T-cells were observed in one case, indicating the presence of immature tertiary lymphoid structures. A positive correlation was observed between the densities of CD4+ and CD8+ T-cells in grade 2 meningiomas but not in grade 1.

Conclusion: The TIME in meningiomas exhibits distinct immune profiles by tumor grade, characterized by the presence of TIL aggregates and coordinated CD4+ and CD8+ T-cell infiltration in higher-grade tumors. These findings may

continued



Dr. Mitsugu Fujita, MD, Ph.D., Center for Medical Education and Clinical Training, Kindai University Faculty of Medicine, 377-2 Ohno-Higashi, Osaka-Sayama, Osaka 589-8511, Japan. Tel: +81 723660221 (Ext 5456), e-mail: mfujita47-umn@umin.ac.jp

Received May 23, 2025 | Revised June 3, 2025 | Accepted June 4, 2025



This is an open access article under the terms of the Creative Commons Attribution License, which permits use, distribution and reproduction in any medium, provided the original work is properly cited.

©2025 The Author(s). Anticancer Research is published by the International Institute of Anticancer Research.

provide insights into the immune landscape of meningiomas and support the development of immunotherapeutic strategies targeting the TIME.

Keywords: Malignant meningioma, tumor immune microenvironment, tumor-infiltrating lymphocytes, B-cells, T-cells.

Introduction

Meningiomas, which arise from the meninges surrounding the brain and spinal cord, are the most common primary intracranial tumors in adults, accounting for approximately 30% of all intracranial tumors (1). They are pathologically classified as grades 1-3 by the World Health Organization classification of tumors of the central nervous system (CNS) (2). More than 90% of meningiomas are benign (grade 1) and can be successfully treated with surgical resection. In contrast, malignant meningiomas (grades 2 and 3) frequently recur despite complete resection and radiotherapy, thereby causing significant morbidity and mortality (3). No effective treatment has been established for these grades to date (4). In recent years, immunotherapy has demonstrated efficacy in several malignancies, highlighting the importance of understanding the tumor immune microenvironment (TIME) (5). However, the role of TIME in meningioma remains largely unknown (6).

TIME is a complex network of tumor, immune and stromal cells as well as intercellular signaling molecules and is involved in tumor progression, immune evasion and treatment response (5). Among them, tumor-infiltrating lymphocytes (TILs), such as CD4⁺ T-, CD8⁺ T- and CD20⁺ B-cells, play a pivotal role in these immune responses. CD4⁺ T-cells can differentiate into different subsets with specialized functions to further control other immune cells. Some CD4⁺ T-cells, known as helper T-lymphocytes, activate CD8⁺ T-cells to promote cellular antitumor immunity. In contrast, a subset of CD4⁺ T-cells, known as regulatory T-cells (Tregs), suppress antitumor immunity and promote tumor growth (7). CD8⁺ T-cells, or cytotoxic T-lymphocytes, are crucial to antitumor immunity; they

can directly kill tumor cells that express specific antigens. Among them, CD8⁺CD103⁺ T-cells are referred to as tissue-resident memory T-cells (TRMs), which persist in peripheral tissues, facilitate rapid immune responses, and provide local immune surveillance (8). CD20⁺ B-cells play a pivotal role in humoral immunity. Tumor-infiltrating B-cells occasionally form lymphoid follicles within tumors, known as tertiary lymphoid structures (TLSs), which enhance antitumor immunity (9). The presence of TLSs has been associated with prognosis in several tumor types.

The balance and interactions between these lymphocyte populations within the TIME can considerably influence tumor growth and treatment response. For example, in glioblastoma, high CD4⁺/CD8⁺ T-cell ratios are associated with poor clinical outcomes (10, 11). Furthermore, pilocytic astrocytoma, a benign CNS tumor, exhibits higher CD8/CD4 ratio than other brain tumors (12). These findings suggest that the balance and interactions between TILs within the TIME differ by tumor types and that understanding the complex intercellular interplay in the TIME is crucial to the development of effective immunotherapeutic strategies for various tumors.

Based on these findings, we hypothesized that TIL distributions and their interactions within the meningioma TIME would influence the biological behavior and clinical outcomes of meningiomas. Considering the heterogeneity of meningiomas, ranging from benign to highly malignant forms, specific immunological characteristics may indicate tumor malignancy. To validate these hypotheses, we investigated the TIME of malignant meningiomas using surgical specimens. Our study focused on the tumor infiltration of immune cells, such as CD4⁺ T-, CD8⁺ T-, and CD20⁺ B-cells, and TRMs.

Patients and Methods

Patients. This study was approved by the institutional ethics review board of Aichi Medical University (AMU; approval number 24-895). The requirement for written informed consent was waived owing to the retrospective nature of the study. Instead, a public notice with information on the study was posted on our hospital's website. All patient identifiers were protected according to ethical guidelines. The study included 22 patients with meningiomas who underwent initial tumor resection at the AMU between January 2014 and December 2023. The patients' age, sex, tumor location, peritumoral edema on preoperative magnetic resonance imaging (MRI), preoperative and postoperative modified Rankin Scale (mRS), follow-up period, recurrence and mortality were evaluated. The mRS is a widely used clinical scale to measure the degree of disability or dependence in patients' daily activities (13). Preoperative mRS was measured on the day before surgery, and postoperative mRS at the last outpatient follow-up visit.

Immunohistochemistry. This procedure has been previously described (14, 15). Briefly, surgical specimens of meningiomas were formalin-fixed, and serial 4- μ m tissue sections were prepared. One of the serial sections was subjected to hematoxylin and eosin staining, and subsequent sections were subjected to immunohistochemistry (IHC) staining. The following monoclonal antibodies (mAbs) were used as primary antibodies for IHC staining: rabbit anti-CD4 mAb (clone EPR6855, Abcam, Cambridge, UK), mouse anti-CD8 mAb (clone C8/144B, DAKO, Glostrup, Denmark), rabbit anti-CD103 mAb (clone EPR4166-2, Abcam), mouse anti-CD20 mAb (clone L26, Nichirei, Tokyo, Japan), and mouse anti-BCL6 mAb (clone LN22, Nichirei). The following secondary antibody complexes were then used: Histofine Simple Stain AP (rabbit, Nichirei) for CD4, Histofine Simple Stain AP (mouse, Nichirei) for CD8, Histofine Simple Stain MAX-PO (rabbit, Nichirei) for CD103, and Histofine Simple Stain MAX-PO (mouse, Nichirei) for CD20 and BCL6. The following substrates were used for the chromogenic

reaction: First Red II Substrate Kit (Nichirei), HistoGreen Substrate Kit (Cosmo Bio, Tokyo, Japan), and Histofine DAB Substrate Kit (Nichirei). Cell nuclei were counterstained with hematoxylin.

Image analysis. This procedure has been previously described (14, 15). Briefly, digital scanning of stained tissue sections was performed using a NanoZoomer-SQ whole slide imaging system (Hamamatsu Photonics, Hamamatsu, Japan) with a 20 \times 0.75 NA objective. Subsequently, the scanned images were imported into QuPath software (ver. 0.5.1) for quantitative analysis. Tumor regions were identified using "pixel classification for automated tissue segmentation" function. Furthermore, cell detection was performed using built-in algorithms of QuPath that automatically analyze color intensity and cell shape. For CD20-, CD4-, and BCL6-stained specimens, the cells were classified into the following seven categories: tumor cells, necrosis, CD4+ T-helper cells, CD4+ monocytes/macrophages, endothelial cells, CD20+ B-cells, and others. For CD8- and CD103-stained specimens, the cells were classified into the following six categories: tumor cells, necrosis, CD103+CD8+ double positive T-cells, CD8+ single positive T-cells, CD103+ single positive cells, and others. Then, the cell classification algorithms were applied to all digital slides to ensure consistent cell classification across cases. Quantitative analysis was also performed, which included measurements of the tumor area and characterization of the classified cells, such as their spatial distribution and morphometric parameters. Regions larger than 250 \times 250 μ m with dense CD20+ B- or CD4+ T-cells were grossly counted as TIL aggregates. These densities were calculated as the number of objects (cells or TIL aggregates) per 1 mm² of tumor area.

Statistical analysis. Statistical analyses were performed as previously described (16, 17). Briefly, the EZR software (version 1.68, Saitama Medical Center, Jichi Medical University, Saitama, Japan) was used for all statistical analyses. The Mann-Whitney *U*-test and Fisher's exact test were used for intergroup comparisons. Pearson's

Table I. Clinical characteristics of patients with meningioma.

	Grade 1 (n=12)	Grade 2 (n=10)	p-Value
Median age (range)	61 (47-82)	72.5 (47-91)	0.64
Female sex (%)	10 (83.3)	5 (50.0)	0.17
Site (%)			
Convexity	6 (50.0)	5 (50.0)	0.26
Cavernous sinus	0 (0.0)	1 (10.0)	
Falx	0 (0.0)	1 (10.0)	
Frontal base	1 (8.3)	1 (10.0)	
Petroclival	4 (33.3)	0 (0.0)	
Sphenoid ridge	0 (0.0)	1 (10.0)	
Parasagittal	1 (8.3)	1 (10.0)	
Preoperative edema on MRI (%)	3 (25.0)	8 (80.0)	0.03*
Preoperative mRS (%)			
0	3 (25.0)	1 (10.0)	0.74
1	6 (50.0)	5 (50.0)	
2	3 (25.0)	2 (20.0)	
3	0 (0.0)	1 (10.0)	
4	0 (0.0)	1 (10.0)	
Postoperative mRS (%)			
0	10 (83.3)	3 (30.0)	0.04*
1	2 (16.7)	2 (20.0)	
2	0 (0.0)	2 (20.0)	
3	0 (0.0)	1 (10.0)	
4	0 (0.0)	2 (20.0)	
Recurrence (%)	0 (0.0)	1 (10.0)	0.46
Death (%)	0 (0.0)	0 (0.0)	NA

mRS: Modified Rankin Scale; NA: not available. * $p < 0.05$.

correlation coefficient was calculated to evaluate the association between two parameters. The threshold for statistical significance was set to $p < 0.05$.

Results

Clinical characteristics of patients with meningioma. We first compared patient characteristics between grade 1 and 2 meningiomas (Table I). There were no significant differences in age, sex, tumor location, preoperative and postoperative mRS, follow-up period, or recurrence rate between the groups. No death occurred in the study cohort. Grade 2 meningiomas were significantly associated with peritumoral edema on preoperative MRI ($p = 0.03$). Postoperative mRS was higher in grade 2 meningiomas ($p = 0.041$) than grade 1 meningiomas,

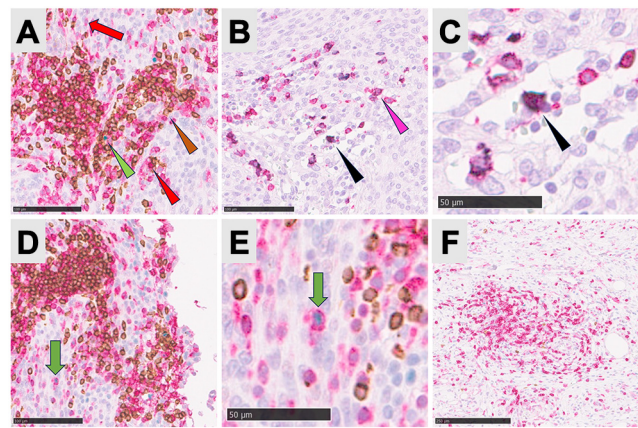


Figure 1. Diverse immune cells constitute the meningioma TIME. (A) Representative image of CD4 (red), CD20 (brown), and BCL-6 (green) triple immunostaining. Red arrow, CD4+ monocytes/macrophages; red arrowhead CD4+ T-cells; brown arrowhead, CD20+ B-cells; green arrowhead, BCL-6+ T-cells. (B) Representative image of CD8 (red) and CD103 (green) double immunostaining. Pink arrowhead, CD8+ T-cells; black arrowhead, CD8+ CD103+ tissue-resident memory T-cells (TRMs). (C) Magnified image of the TRM in Figure B. (D) TIL aggregation composed of abundant CD20+ B-cells. Green arrow, CD4+ BCL-6+ follicular helper T-cells (Tfh). (E) Magnified image of the Tfh-cell in Figure D. The cell nuclei are positive for BCL-6 (green), and the surrounding cell membranes are positive for CD4 (red). (F) TIL aggregation mainly composed of CD4+ T-cells. Scale bar, 100 μm (A, B, and D), 50 μm (C and E), and 250 μm (F).

indicating a significantly poor neurological functional outcome.

Diverse immune cells constitute the meningioma TIME. We then attempted to detect immune cells in the meningioma TIME. Through multicolor IHC, CD4+ and CD20+ cells were detected at a high frequency, whereas very few BCL-6+ cells were sparsely observed (Figure 1A). The deep learning cell classification function of QuPath appropriately distinguished CD4+ T-cells from CD4+ monocytes/macrophages based on their distinct morphological features and staining intensity patterns; the monocytes/macrophages exhibited weak CD4 expression with a large cytoplasm (Figure 1A, red arrows), whereas the lymphocytes showed strong CD4 expression with small, round morphology (Figure 1A, red arrowheads). In addition, we detected CD8+ cells (Figure 1B) and their subpopulation CD8+CD103+ double positive TRMs (Figure 1C). We then searched for TIL aggregates in the meningioma

Table II. *Densities of tumor-infiltrating lymphocytes (TILs) and TIL aggregates in the meningioma TIME.*

No.	Age	Sex	Grade	CD4+ M/M density (/mm ²)	CD4+ T-cell density (/mm ²)	CD8+ T-cell density (/mm ²)	TRM density (/mm ²)	CD20+ B-cell density (/mm ²)	TIL aggregate density (/cm ²)
1	63	F	1	279.724	82.04	25.436	0	6.252	0
2	59	F	1	122.281	27.006	44.329	0.57	2.661	0
3	58	F	1	187.839	20.91	26.128	0.037	0.549	0
4	47	F	1	64.469	23.437	43.84	0.093	1.483	0
5	75	F	1	287.082	26.858	19.617	0.186	0.291	0
6	82	F	1	202.114	41.875	16.471	0	1.033	0
7	55	M	1	178.042	33.853	33.447	0.119	1.426	0
8	79	F	1	98.955	27.499	4.671	0.038	0.634	0
9	71	F	1	537.138	46.916	19.406	0.119	3.202	0
10	65	F	1	517.542	21.338	11.95	0.005	1.691	0
11	56	F	1	99.538	27.815	12.515	0.091	5.655	0
12	58	M	1	176.602	26.663	45.831	0.306	2.134	0
13	51	F	2	175.556	12.255	37.152	0.049	0.508	0
14	47	M	2	333.792	298.49	148.004	0.318	14.673	2.877
15	51	F	2	667.414	135.685	70.668	1.541	53.846	28.859
16	79	F	2	684.229	15.104	7.884	0.021	0.617	0
17	58	M	2	264.693	32.728	109.482	1.766	5.674	0.494
18	76	M	2	378.896	29.534	20.711	0.158	1.012	0
19	74	M	2	63.609	55.405	19.67	0.088	0.764	0
20	91	F	2	283.299	16.544	2.759	0.011	0.628	0
21	71	M	2	80.765	66.867	96.96	0.063	2.126	0
22	79	F	2	49.398	174.414	67.584	0.069	5.566	0.736

CD4+ M/M: CD4+ monocytes/macrophages; TRM: tissue-resident memory T-cell; TIL: tumor-infiltrating lymphocyte.

TIME. In one case of grade 2 meningioma, we detected cluster-like aggregates mainly composed of abundant CD20+ B-cells with some CD4+BCL-6+ follicular helper T-cells (Tfh) around the cluster (case 15; Figure 1D and E). In some grade 2 cases, we also detected TIL aggregates composed of CD4+ T- and CD20+ B-cells surrounded by CD4+ monocytes/macrophages (Figure 1F). In contrast, no such structures were detected in grade 1 cases (data not shown).

Densities of TIL aggregates in the meningioma TIME correlate with pathological tumor grades. Based on the above data, we summarized the detailed information of these TIL subsets per tumor grade (Table II); BCL-6+ cells were not analyzed owing to their paucity. There was no significant difference in the densities of CD4+ monocytes/macrophages (Figure 2A), CD4+ T-cells (Figure 2B), CD8+ T-cells (Figure 2C), CD8+CD103+ TRMs (Figure 2D), and CD20+ B-cells (Figure 2E) per tumor grade. In

contrast, the density of TIL aggregates significantly correlated with tumor grade ($p=0.02$; Figure 2F). These data suggest that while the densities of each TIL subset in the meningioma TIME are irrelevant to pathological tumor grades, those of immunoreactive structures, such as TIL aggregates, would correlate with pathological malignancy and thus robust immune responses.

We also analyzed whether the densities of each TIL subset or TIL aggregates would correlate with the prognosis of our meningioma cases. As no death occurred in the study cohort, we used postoperative mRS as a measure of neurological function for this purpose. However, no significant difference was observed in these parameters (data not shown).

The density ratios of CD4+ T- and CD8+ T-cells correlate in grade 2 meningiomas. After observing the activation of potent antitumor immunity in grade 2 meningiomas (Figure 2F), we investigated the interactions between

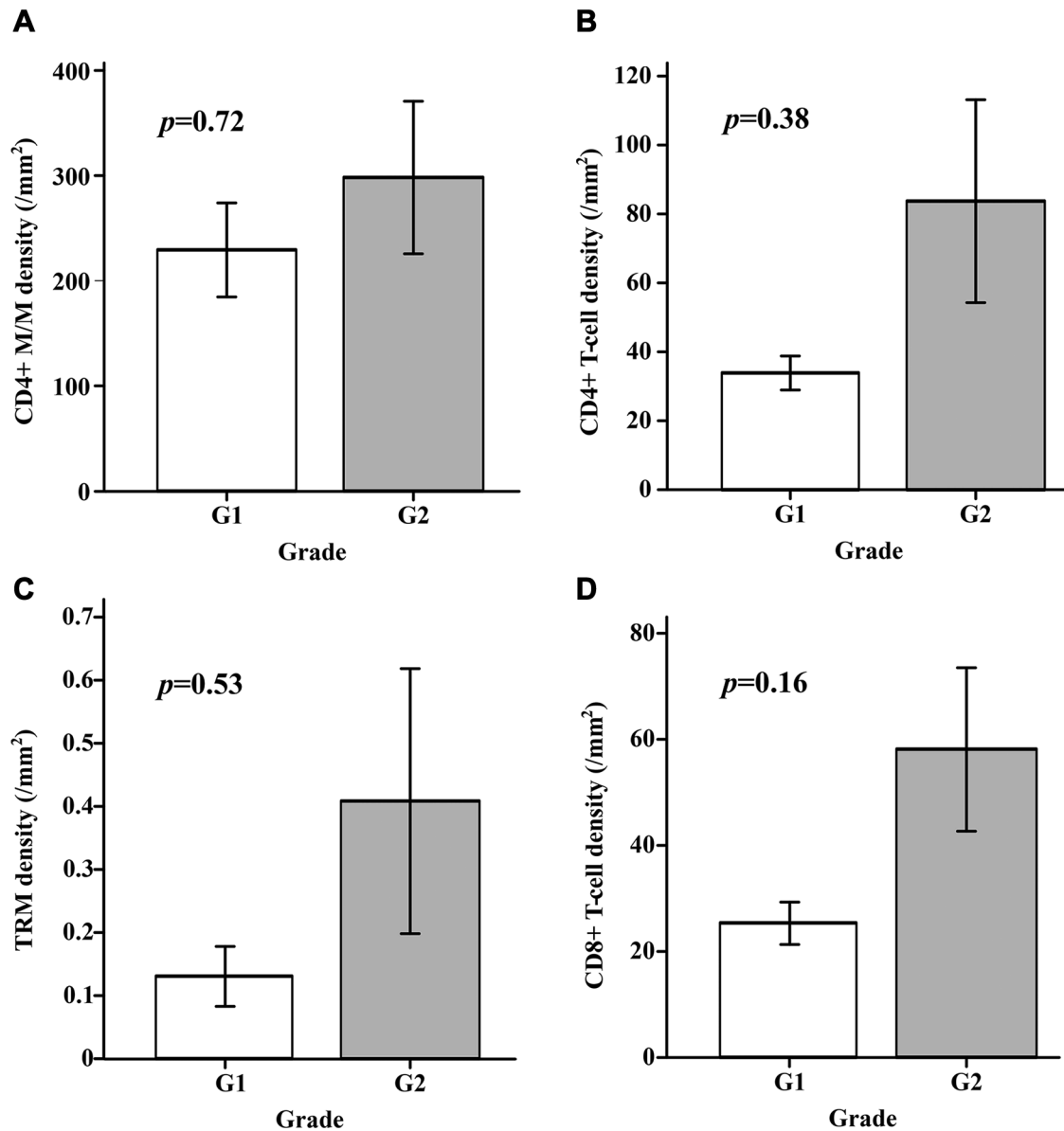


Figure 2. Continued

different TIL subsets across tumor grades. As a result, the densities of CD4+ T- and CD8+ T-cells did not correlate in grade 1 ($p=0.80$; Figure 3A) but positively correlated in grade 2 ($p=0.02$; Figure 3B). No other TIL combinations showed any correlation (data not shown). In conclusion, our data suggest that the meningioma TIME exhibits distinct patterns with TIL aggregates and coordinated

CD4+ and CD8+ T-cell infiltration, which may reveal new therapeutic targets for these diseases.

Discussion

In this study, we aimed to characterize the composition of meningioma TIME. To this end, we retrospectively

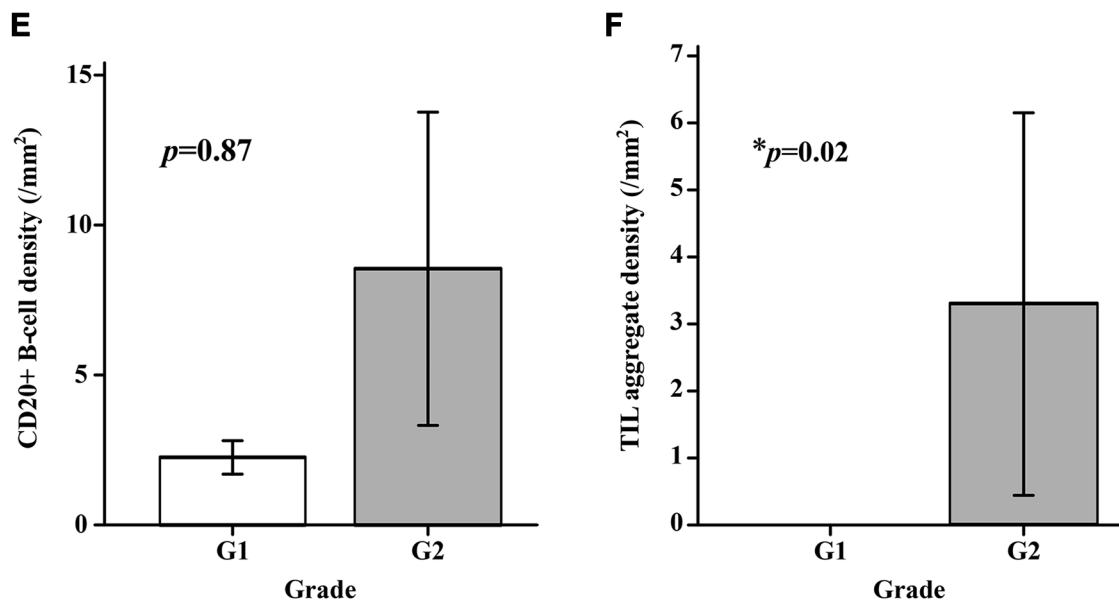


Figure 2. The densities of TIL aggregates in the meningioma TIME correlate with pathological tumor grades. (A) CD4+ monocyte/macrophages, (B) CD4+ T-cells, (C) CD8+ T-cells, (D) tissue-resident memory T-cells (TRMs), (E) CD20+ B-cells, and (F) TIL aggregates.

collected our cohort (Table I) and performed pathological analyses using multicolor IHC and the QuPath software. As a result, we observed diverse immune cells constituting the meningioma TIME (Figure 1 and Table II). Although the densities of individual TIL subsets did not correlate with the tumor grades (Figure 2), those of TIL aggregates showed correlation (Figure 2F). However, these data did not correlate with postoperative neurological function (data not shown). We then examined the interactions between different TIL subsets per tumor grade (Figure 3). As a result, the densities of CD4+ T- and CD8+ T-cells were well correlated, particularly in grade 2 meningiomas (Figure 3B). Taken together, these data suggest that the components of meningioma TIME would differ by tumor grade, with more coordinated CD4+ and CD8+ T-cell infiltrations in higher-grade meningiomas.

In one case of grade 2 meningioma, we observed TIL aggregates accompanied by CD4+BCL-6+ Tfh-cells (Figure 1D and E), which we believe are relevant to TLS as described below. TLS are classified into three types based on maturation status: immature TLS, primary follicle-like

TLS, and secondary follicle-like TLS (mature TLS) (18, 19). Immature TLS are characterized by T- and B-cell aggregates that lack B-cell follicles and CD21+ follicular dendritic cells (FDCs). Primary follicle-like TLS are characterized by the presence of FDCs within the B-cell zone. Mature TLS is characterized by the formation of germinal centers, primarily composed of CD20+BCL-6+ B- and Tfh-cells (20). Our observation that Tfh-cells were present around the TIL aggregates rather than in the center suggests that these structures would represent immature TLS. Although we have recently demonstrated the presence and importance of TLS in the CNS metastases of lung cancer (14) and gastrointestinal cancer (15), studies on TLS in the meningioma TIME remain scarce. Further studies are needed to clarify their characteristics and functional significance in meningiomas.

In contrast to grade 1 meningiomas, grade 2 meningiomas exhibited a positive correlation between the CD4+ and CD8+ T-cell densities (Figure 3). This difference suggests an alteration in the immune responses between these tumor grades. In fact, the immune responses within

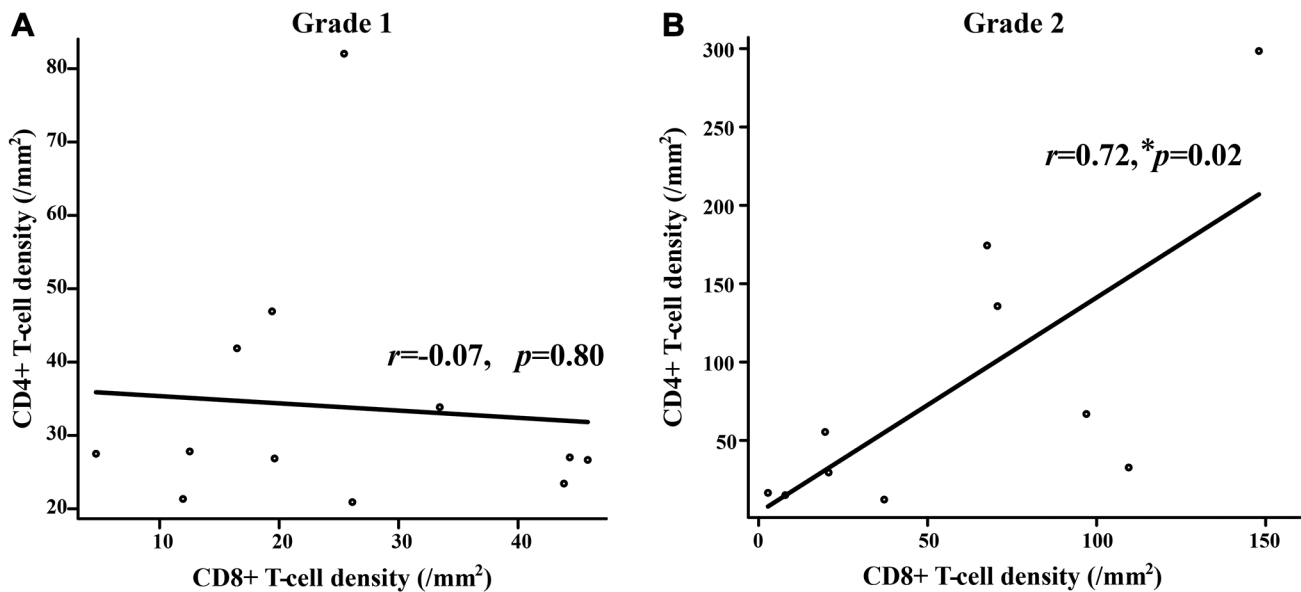


Figure 3. The density ratios of CD4+ T- and CD8+ T-cells are correlated in grade 2 meningiomas. (A) grade 1 and (B) grade 2 meningiomas.

the TIME would vary according to tumor type and progression status (21). In glioblastoma, which is the most common CNS malignancy, the ratio of FoxP3+ Tregs to CD4+ helper T-cells correlates with tumor recurrence and patient survival (10, 11). In pediatric CNS tumors, such as pilocytic astrocytoma, higher CD8/CD4 ratios in the TIME than in normal brain tissues suggest selective recruitment of CD8+ T-cells into the TIME (11). In the meningioma TIME, CD8+ T-cells have been reported to predominate over CD4+ T-cells (22). However, little attention has been paid to the correlation between CD4+ and CD8+ T-cells, which renders our findings important in the meningioma TIME. Although our findings merely demonstrate a positive correlation between CD4+ and CD8+ T-cell densities in grade 2 meningioma tissues without clarifying the underlying mechanisms of tumor progression control, they may provide new evidence that the meningioma TIME evolves with tumor progression and thus offer new immunological therapeutic targets for higher-grade meningiomas.

Study limitations. The relatively small sample size (n=22) and short follow-up periods limited the statistical analyses.

As there were no fatal cases, which is clinically favorable, prognostic analyses were severely limited. Although we performed the Mann-Whitney *U*-test to analyze the density of TIL aggregates, the results should be interpreted with caution as TIL aggregates were absent in grade 1 meningiomas. Furthermore, the non-consecutive selection of grade 1 meningiomas may have introduced a potential selection bias. Future studies with larger cohorts and functional analyses of TIME are needed to validate our findings regarding immunohistopathology in meningioma.

Conclusion

This study characterized the meningioma TIME and showed that while individual TIL densities did not correlate with tumor grade, the presence of TIL aggregates significantly correlated with higher-grade meningiomas. A positive correlation was observed between CD4+ and CD8+ T-cell densities in grade 2 meningiomas, suggesting more coordinated immune responses in higher-grade tumors. The identified TIL aggregates accompanied by Tfh-cells in grade 2 meningiomas likely represent immature

TLS, although their functional significance requires further investigation.

Conflicts of Interest

The Authors declare no conflicts of interest in relation to this study.

Authors' Contributions

TI, EI, MO, SK, and MF conceptualized the project. EI, MO, SK, and TN acquired the funding. MO and MF supervised the project and conducted the project administration. TI, EI, and TW provided resources. MO, TN, and MF developed the methodology. TI and EI acquired raw data. TI, EI, and MF carried out formal analyses. TI and EI wrote the original draft. MO, SK, TN, and MF edited the manuscript. All the Authors have reviewed and approved the final manuscript.

Acknowledgements

The Authors would like to thank Aichi Pathological Diagnostic Clinic (aichi-path-cl.com) for the IHC staining and Enago (enago.jp) for the English language review.

Funding

This work was supported by JSPS KAKENHI (22K09223 to MO, 23K15677 to SK, 24K10381 to TN, and 24K12219 to EI).

Artificial Intelligence (AI) Disclosure

During the preparation of this manuscript, ChatGPT, Perplexity, and DeepL were used solely for language editing and stylistic improvements in select paragraphs. No sections involving the generation, analysis, or interpretation of research data were produced by generative AI. All scientific content was created and verified by the authors. Furthermore, no figures or visual

data were generated or modified using generative AI or machine learning-based image enhancement tools.

References

- Ostrom QT, Cioffi G, Waite K, Kruchko C, Barnholtz-Sloan JS: CBTRUS statistical report: Primary brain and other central nervous system tumors diagnosed in the United States in 2014-2018. *Neuro Oncol* 23(12 Suppl 2): iii1-iii105, 2021. DOI: 10.1093/neuonc/noab200
- Louis DN, Perry A, Wesseling P, Brat DJ, Cree IA, Figarella-Branger D, Hawkins C, Ng HK, Pfister SM, Reifenberger G, Soffietti R, von Deimling A, Ellison DW: The 2021 WHO Classification of Tumors of the Central Nervous System: a summary. *Neuro Oncol* 23(8): 1231-1251, 2021. DOI: 10.1093/neuonc/noab106
- Violaris K, Katsarides V, Karakyriou M, Sakellariou P: Surgical outcome of treating grades II and III meningiomas: a report of 32 cases. *Neurosci J* 2013: 706481, 2013. DOI: 10.1155/2013/706481
- Mair MJ, Berghoff AS, Brastianos PK, Preusser M: Emerging systemic treatment options in meningioma. *J Neurooncol* 161(2): 245-258, 2023. DOI: 10.1007/s11060-022-04148-8
- Binnewies M, Roberts EW, Kersten K, Chan V, Fearon DF, Merad M, Coussens LM, Gabrilovich DI, Ostrand-Rosenberg S, Hedrick CC, Vonderheide RH, Pittet MJ, Jain RK, Zou W, Howcroft TK, Woodhouse EC, Weinberg RA, Krummel MF: Understanding the tumor immune microenvironment (TIME) for effective therapy. *Nat Med* 24(5): 541-550, 2018. DOI: 10.1038/s41591-018-0014-x
- Garzon-Muvdi T, Bailey DD, Pernik MN, Pan E: Basis for immunotherapy for treatment of meningiomas. *Front Neurol* 11: 945, 2020. DOI: 10.3389/fneur.2020.00945
- Scott EN, Gocher AM, Workman CJ, Vignali DAA: Regulatory T cells: barriers of immune infiltration into the tumor microenvironment. *Front Immunol* 12: 702726, 2021. DOI: 10.3389/fimmu.2021.702726
- Masopust D, Soerens AG: Tissue-resident T cells and other resident leukocytes. *Annu Rev Immunol* 37: 521-546, 2019. DOI: 10.1146/annurev-immunol-042617-053214
- Sautès-Fridman C, Petitprez F, Calderaro J, Fridman WH: Tertiary lymphoid structures in the era of cancer immunotherapy. *Nat Rev Cancer* 19(6): 307-325, 2019. DOI: 10.1038/s41568-019-0144-6
- Han S, Zhang C, Li Q, Dong J, Liu Y, Huang Y, Jiang T, Wu A: Tumour-infiltrating CD4(+) and CD8(+) lymphocytes as predictors of clinical outcome in glioma. *Br J Cancer* 110(10): 2560-2568, 2014. DOI: 10.1038/bjc.2014.162
- Sayour EJ, McLendon P, McLendon R, De Leon G, Reynolds R, Kresak J, Sampson JH, Mitchell DA: Increased proportion of FoxP3+ regulatory T cells in tumor infiltrating lymphocytes is associated with tumor recurrence and

- reduced survival in patients with glioblastoma. *Cancer Immunol Immunother* 64(4): 419-427, 2015. DOI: 10.1007/s00262-014-1651-7
- 12 Griesinger AM, Birks DK, Donson AM, Amani V, Hoffman LM, Waziri A, Wang M, Handler MH, Foreman NK: Characterization of distinct immunophenotypes across pediatric brain tumor types. *J Immunol* 191(9): 4880-4888, 2013. DOI: 10.4049/jimmunol.1301966
 - 13 Banks JL, Marotta CA: Outcomes validity and reliability of the modified rankin scale: implications for stroke clinical trials. *Stroke* 38(3): 1091-1096, 2007. DOI: 10.1161/01.STR.0000258355.23810.c6
 - 14 Nohira S, Kuramitsu S, Ohno M, Fujita M, Yamashita K, Nagasaka T, Haimoto S, Sakakura N, Matsushita H, Saito R: Tertiary lymphoid structures in brain metastases of lung cancer: prognostic significance and correlation with clinical outcomes. *Anticancer Res* 44(8): 3615-3621, 2024. DOI: 10.21873/anticancer.17184
 - 15 Ohno M, Kuramitsu S, Yamashita K, Nagasaka T, Haimoto S, Fujita M: Tumor-infiltrating B cells and tissue-resident memory T cells as prognostic indicators in brain metastases derived from gastrointestinal cancers. *Cancers (Basel)* 16(22): 3765, 2024. DOI: 10.3390/cancers16223765
 - 16 Kanda Y: Investigation of the freely available easy-to-use software 'EZR' for medical statistics. *Bone Marrow Transplant* 48(3): 452-458, 2013. DOI: 10.1038/bmt.2012.244
 - 17 Okuda T, Fujita M, Kato A: Significance of elevated HMGB1 expression in pituitary apoplexy. *Anticancer Res* 39(8): 4491-4494, 2019. DOI: 10.21873/anticancer.13624
 - 18 Bao X, Lin X, Xie M, Yao J, Song J, Ma X, Zhang X, Zhang Y, Liu Y, Han W, Liang Y, Hu H, Xu L, Xue X: Mature tertiary lymphoid structures: important contributors to anti-tumor immune efficacy. *Front Immunol* 15: 1413067, 2024. DOI: 10.3389/fimmu.2024.1413067
 - 19 N J, J T, Sl N, Gt B: Tertiary lymphoid structures and B lymphocytes in cancer prognosis and response to immunotherapies. *Oncoimmunology* 10(1): 1900508, 2021. DOI: 10.1080/2162402X.2021.1900508
 - 20 Qin M, Jin Y, Pan LY: Tertiary lymphoid structure and B-cell-related pathways: A potential target in tumor immunotherapy. *Oncol Lett* 22(6): 836, 2021. DOI: 10.3892/ol.2021.13097
 - 21 Quail DF, Joyce JA: Microenvironmental regulation of tumor progression and metastasis. *Nat Med* 19(11): 1423-1437, 2013. DOI: 10.1038/nm.3394
 - 22 Fang L, Lowther DE, Meizlish ML, Anderson RC, Bruce JN, Devine L, Huttner AJ, Kleinstein SH, Lee JY, Stern JN, Yaari G, Lovato L, Cronk KM, O'Connor KC: The immune cell infiltrate populating meningiomas is composed of mature, antigen-experienced T and B cells. *Neuro Oncol* 15(11): 1479-1490, 2013. DOI: 10.1093/neuonc/not110